# Effects of formalin fixing on the terahertz properties of biological tissues

**Yiwen Sun**
The Chinese University of Hong Kong
Department of Electronic Engineering
Shatin, N.T., Hong Kong

**Bernd M. Fischer**
The University of Adelaide
School of Electrical and Electronic Engineering
North Terrace Campus
Adelaide, SA 5005
Australia
and
French-German Research Institute of Saint Louis
Div IV (ERG), France

**Emma Pickwell-MacPherson**
The Chinese University of Hong Kong
Department of Electronic Engineering
Shatin, N.T., Hong Kong

**Abstract.** We demonstrate how the terahertz properties of porcine adipose tissue and skeletal muscle are affected by formalin fixing. Terahertz radiation is sensitive to covalently cross-linked proteins and can be used to probe unique spectroscopic signatures. We study in detail the changes arising from different fixation times and see that formalin fixing reduces the refractive index and the absorption coefficient of the samples in the terahertz regime. These fundamental properties affect the time-domain terahertz response of the samples and determine the level of image contrast that can be achieved. © *2009 Society of Photo-Optical Instrumentation Engineers.* [DOI: 10.1117/1.3268439]

Keywords: terahertz pulsed imaging; terahertz spectroscopy; formalin-fixed; biological samples; time domain; frequency domain.

Paper 09150R received Apr. 17, 2009; revised manuscript received Sep. 11, 2009; accepted for publication Sep. 22, 2009; published online Dec. 2, 2009.

## 1 Introduction

Now that the hurdle of generating terahertz radiation has been overcome,[1] there is increasing interest in the terahertz (THz $=10^{12}$ Hz) region in applications ranging from pharmaceuticals[2,3] to dental[4] and medical imaging.[5,6] In this paper, we define the THz range as 100 GHz to 10 THz. THz radiation is nonionizing, nondestructive, and noninvasive:[7,8] the low energy of the THz radiation does not damage the sample.[9] Toward the higher frequency end of the THz range (from ~1 THz and above), there are vibrational modes corresponding to protein tertiary structural motion: such intermolecular interactions are present in many biomolecules. Other molecular properties that can be probed in the THz range include bulk dielectric relaxation modes[10] and phonon modes[11]—these can be difficult to probe using other techniques. For instance, nuclear magnetic resonance spectroscopy can determine the presence of various carbon bonds; however, it cannot be used to distinguish between molecules with the same molecular formula, but different structure (isomers).[12] THz spectroscopy is able to distinguish between isomers and polymorphs[13] and is therefore emerging as an important and highly sensitive tool to determine biomolecular structure and dynamics.[14,15] Indeed, THz spectroscopy can distinguish between two types of artificial ribonucleic acid (RNA) strands when measured in dehydrated form.[16] Furthermore Fischer et al. demonstrated that even when the molecular structure only differs in the direction of a single hydroxyl group with respect to the ring plane, a pronounced difference in the THz spectra is observed.[17] Intermolecular interactions are present in all biomolecules, and because biomolecules are the fundamental components of biological samples, they can be used to provide a natural source of image contrast in biomedical THz imaging.[18]

Several THz studies of freshly excised tissue have highlighted the sensitivity of THz imaging to biological tissues. For instance, THz images of skin cancer have shown contrast between healthy and diseased areas.[18] The contrast can be attributed to differences in the fundamental properties of the tissues:[19] diseased skin tissue (basal cell carcinoma) has been found to have an increased absorption coefficient compared to the adjacent normal tissue.[20] In a breast cancer study, THz images of freshly excised human breast tissue revealed tumor margins that correlated well with those from histology,[6] and recent THz reflection spectroscopy of freshly excised rat tissues has been able to distinguish between healthy tissues from different organs.[21] However, it is not always possible to obtain fresh samples for a study; the most common preservation technique is formalin fixing.

Formalin fixing is used to preserve tissues for routine histopathological diagnosis, and the resulting samples are often useful for retrospective studies. However, along with sample variability, the sample distortion caused by formalin fixing can present challenges. For example, DNA information is often spoiled by the fixing process.[22] Previous THz images of histopathological samples have been able to reveal contrast between different tissue types. Knobloch et al. imaged formalin-fixed and paraffin-embedded samples in transmission geometry, and contrast between the soft tissue and the cartilage of a pig larynx was seen at particular frequency windows.[23] Similarly, they observed contrast between the healthy and diseased areas in an image of a histopathological human liver sample with metastasis. However, it would be useful to know if there would have been more THz contrast if

Address all correspondence to: Emma Pickwell-MacPherson, The Chinese University of Hong Kong, Department of Electronic Engineering, Shatin, N.T. Hong Kong. Tel: 852 26098260; E-mail: e.pickwell.97@cantab.net

1083-3668/2009/14(6)/064017/7/$25.00 © 2009 SPIE

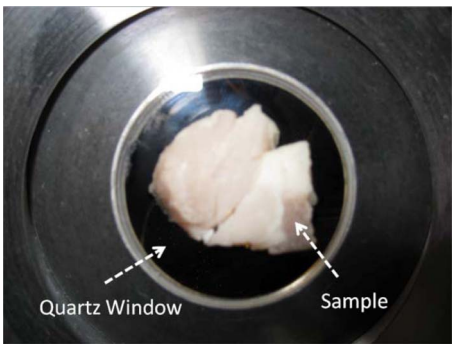


**Fig. 1** Photograph of a sample to be imaged placed on the quartz window.

the samples had been measured fresh, or conversely if the fixing process had enhanced the THz contrast.

In this paper, we present a controlled study to investigate the effects of formalin fixing on the THz properties of two different tissue types (porcine adipose tissue and muscle). The optical properties of fresh and formalin-fixed samples in the THz frequency range were measured using THz reflection spectroscopy. The results are compared, and we discuss how the fixing process can affect image contrast in THz images of biological samples.

## 2 Experimental Methods

### 2.1 *Imaging System*

The THz pulsed imaging (TPI™) system used in this study was the TPI Imaga 1000™ (TeraView Limited, Cambridge, United Kingdom). Detailed information about the system can be found in our previous work.[24–26] Briefly, the system uses photoconductive devices to generate and detect THz light: the optical excitation is achieved by an 800-nm femtosecond pulsed laser. The system has a reflection geometry such that the THz pulses are collimated and focused using off-axis parabolic mirrors onto the top surface of a $z$-cut 2-mm-thick quartz window with an angle of incidence of 30 deg. The sample is placed on the quartz window, and the reflected THz pulse from the quartz/sample interface is detected coherently by a photoconductive receiver. In this system, the relaxation of the excited carriers produced broadband electromagnetic pulses typically with a full width at half maximum of 0.3 ps and results in a usable frequency range from about 0.1 to 3 THz with an average power of $\sim 1\ \mu$W. The THz beam path was purged with nitrogen gas to remove water vapor from the air, which would otherwise have attenuated the signal.[27] Figure 1 is a photograph of a tissue sample placed on the quartz window of our system.

### 2.2 *Sample Preparation*

Three samples of white adipose tissue and two samples of porcine skeletal muscle were taken from the same piece of meat for investigation. The meat was from an abattoir and stored in a refrigerator, it was first measured within 24 h of collection. Adipose tissue was chosen because fatty tissue is known to have significantly different THz properties from other more fibrous/lean tissues; this means that it should be easier to see the contrast before and during the fixing process. The focus of this study was to see how fixing can affect THz image contrast—we are investigating intrasubject variation rather than subject-to-subject (or intersubject) variation. Thus, by taking all the samples from the same piece of meat, we were able to study the effects of the fixation process without added subject variation. The samples were therefore all treated and handled in the same way and exposed to the same environmental conditions. THz radiation can penetrate through several millimeters of some dehydrated tissues;[25–28] therefore, to avoid potential etaloning within the sample after the fixing, each sample was cut such that the thinnest dimension was no less than 1 cm in thickness. The fresh samples were imaged before the formalin-fixing process began. A standard protocol was followed for this process,[29,30] whereby non-buffered 30% formalin was used. The volume of formalin applied to the sample was at least 20 times the initial sample volume. The sample was then left to soak in the fixative in a sealed container and refrigerated at a constant temperature (4 °C). The penetration of formalin is related to the temperature of the solution,[31] and thus, great care was taken to store all samples and formalin at the same temperature. Before placing the fixed tissue sample to be measured on the quartz window, the sample was washed under running water for 20 min to remove the excess formalin and then dried using blotting paper. During imaging, gentle pressure was applied to the sample to ensure it made good contact with the quartz.[20] This became more difficult as the fixing progressed because the sample became more rigid. In order to monitor the changes caused by the formalin, each sample was measured after being fixed for 24, 48, and 72 h. Only data points where the sample had made good contact with the quartz window were used in the following results.

## 3 Results and Discussion

### 3.1 *Frequency-Domain Analysis*

The raw THz data obtained by our system are in the time domain. However, because the fundamental optical properties of interest, namely, the refractive index and absorption coefficient, are frequency dependent, we present the frequency domain analysis first.

By Fourier transforming the sample data and applying Fresnel equations to both sample and reference data, as detailed in Ref. 21, the refractive index and absorption coefficient were calculated. The reflection off the quartz/air interface was used as the reference data throughout this study. The calculated mean refractive index and mean absorption coefficient from the fresh and fixed sample measurements over time are plotted in Figs. 2 and 3 for the muscle and adipose tissue samples, respectively. Data for water and formalin are also plotted for comparison. In Fig. 4, we plot the mean refractive index and mean absorption coefficient from the adipose tissue and skeletal muscle samples for both when the samples were fresh and also after 72 h of formalin fixing. Following standard statistical methods, we calculate the 95% confidence intervals[32] for the tissue samples by averaging over all samples of each tissue type (a total of $>500$ data points were used for each tissue type). The confidence intervals are plotted as error bars in Fig. 4 to illustrate that, both before and after fixing, there are statistically significant differences between the THz properties of the tissues (because the error bars do

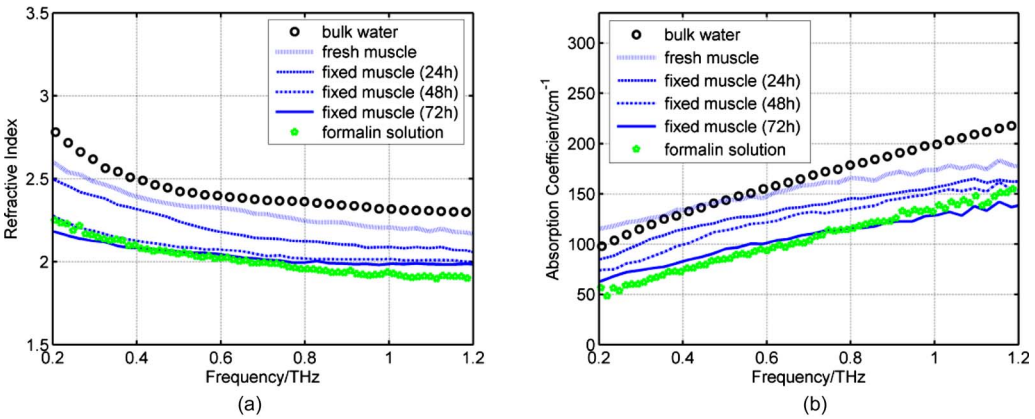


**Fig. 2** (a) The mean refractive index and (b) absorption coefficient of skeletal muscle before and after formalin fixing for 24, 48, and 72 h. Bulk water and formalin optical properties are also plotted for reference.

not overlap). The THz properties of water have also been plotted alongside those of the fresh muscle to highlight that, although the muscle tissue properties are close to those of water, they are significantly different over most of the frequency range investigated.

The refractive index of the skeletal muscle decreased as the fixation time increased and seemed to converge after 48 h. Comparing the fresh and fixed samples, the refractive index changed noticeably at the lower frequencies, falling from 2.6 (fresh) to 2.2 (72 h) at 0.2 THz. From ~0.8 THz and above, the curves of the fixed samples started to plateau toward a refractive index of 2 [Fig. 2(a)]. Because water was being removed from the tissue, it is logical that the absorption coefficient should also be reduced by the fixing process, as shown in Fig. 2. Before fixing, the absorption coefficient of the skeletal muscle tissue was ~120 $cm^{-1}$ at 0.2 THz; it decreased rapidly to 60 $cm^{-1}$ after only 24 h. During the first 24 h, the percentage of moisture being replaced was at its greatest, but as the fixing progressed there was less and less water left to be displaced and so the changes in optical properties decreased and tended toward zero as the fixing time increased. Other studies have also indicated that THz properties are dependent on the sample hydration. For instance, Stringer et al. investigated *ex vivo* samples of human cortical bone and found that dehydrating the sample reduced both the absorption coefficient and the refractive index of the samples.[33]

Similarly, above 0.6 THz, the refractive index and absorption coefficient of the white adipose tissue decreased as the fixation time increased. However, the changes in the adipose tissue refractive index were not as significant as for the muscle. We explain these observations by considering the molecular interactions of the formalin with both muscle and adipose tissue.

Formalin is a saturated solution of formaldehyde (HCHO), water, and methanol. Unlike most antibacterial and germicidal agents, which poison the bacteria and germ cells, formaldehyde kills cell tissue by dehydrating the tissue and bacteria cells and replacing the normal fluid in the cells with a gellike rigid compound.[34] Additionally, the structure of the protein in the "new" cell will resist further bacterial attacks.[35,36] Tissue and bacterium cells are made of protoplasm and, as such, contain large amounts of moisture. Skeletal muscle cells contain several types of protein and have a high water content. The water content in the muscle tissue is about 75–80%,[37] and from Fig. 2, we see that the refractive index and absorption coefficient of the fresh muscle are close to those of water.

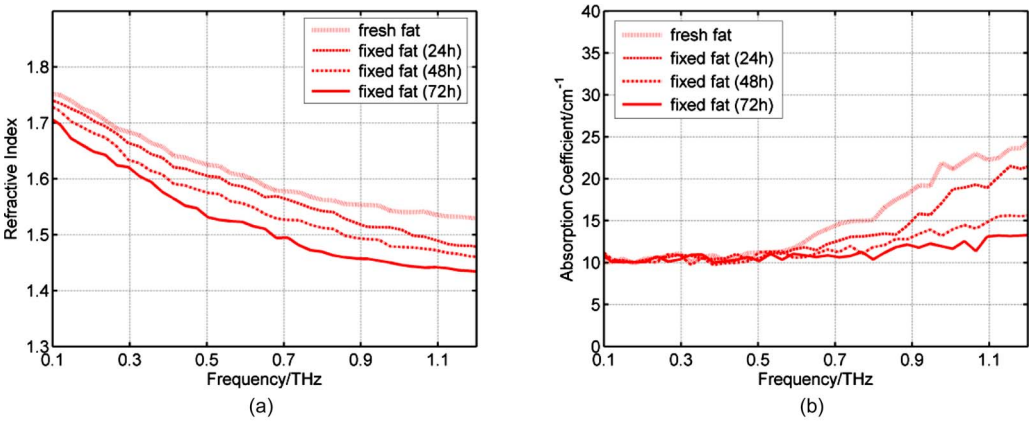


**Fig. 3** (a) The mean refractive index and (b) absorption coefficient of white adipose tissue before and after formalin fixing for 24, 48, and 72 h.

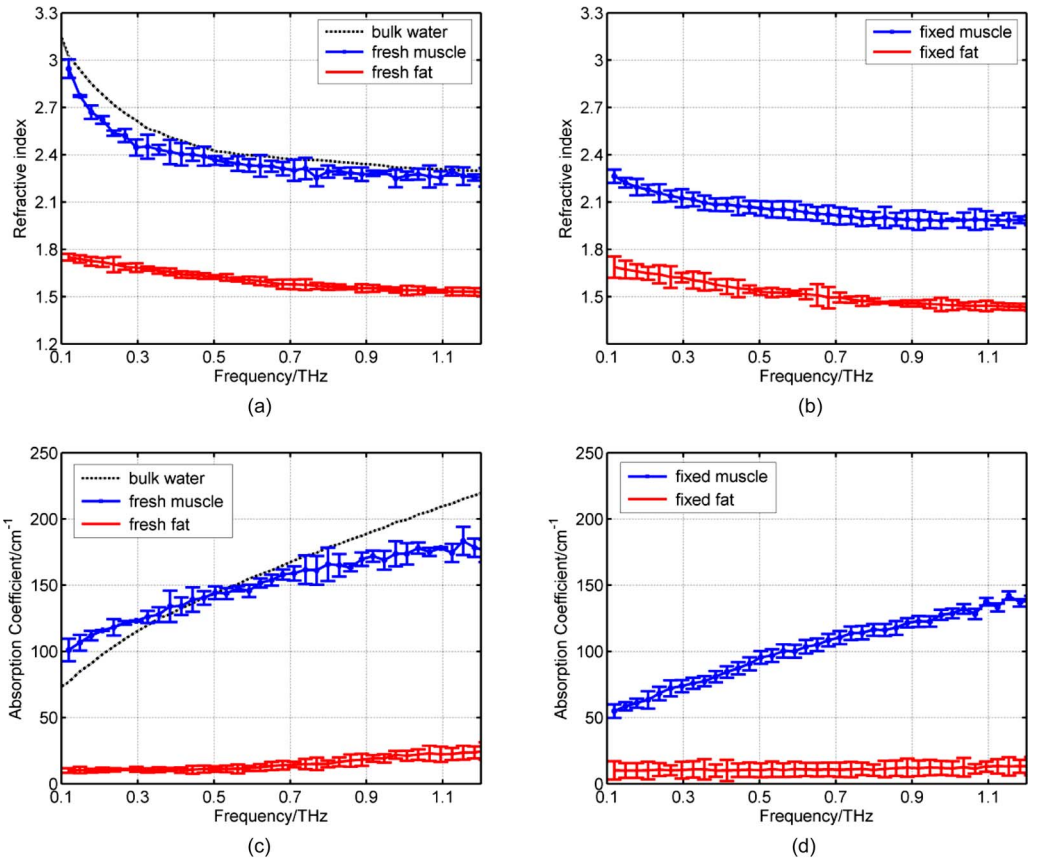


**Fig. 4** The mean refractive index and absorption coefficient for fresh and fixed samples of fat and muscle. Error bars represent 95% confidence intervals. The water data were acquired in transmission, and the error bars are too small to be seen on this graph.

Additionally, the refractive index and absorption coefficient of formalin are much lower than those of water or fresh tissue. The introduction of formaldehyde into the tissue dries out the protoplasm and destroys the cell. Because water is being removed from the tissue, it is logical that the absorption coefficient should be reduced by the fixing process. Similarly, the refractive index is also reduced and becomes closer to that of formalin. In contrast to the muscle tissue, white adipose tissue cells contain a single large fat droplet and the water content is about 10–30%,[37] which is far less than the muscle tissue. This means there is very little water for the formaldehyde to displace, and thus, we do not see such significant changes in the THz properties of the adipose tissue.

### 3.2 *Time-Domain Analysis*

The amplitude and phase of a THz pulse reflected off a medium are dependent on the complex refractive index of the medium (as well as the incident pulse). As in optics, if a THz pulse is reflected by a medium of higher refractive index, then it incurs a phase change of 180 deg. Conversely, if a THz pulse is reflected by a medium of lower refractive index, then there is no phase change. Given that in Section 3.1 we have seen changes in the refractive index and absorption coefficients of the samples during the fixing process, we also expect to see changes in the reflected THz pulses.

To analyze the reflected time-domain pulses meaningfully, the system response was removed. This was done by deconvolving the sample pulse by the reference pulse and applying a bandpass (double Gaussian) filter to reduce the noise as detailed in our previous work.[25] The resulting waveforms for the three fresh adipose tissue samples and two fresh skeletal muscle samples and their corresponding means are illustrated in Fig. 5. From Fig. 5, we see that there is some variation between samples from the same type of tissue but that this variation is slight. In Fig. 6, we illustrate the effects of the formalin fixing by plotting the mean deconvolved waveforms of each tissue type.

As seen in Fig. 6(a), when the fixing time increased, the waveform amplitude of the adipose tissue also increased. This was primarily because the refractive index of the adipose [Fig. 3(a)] was decreasing over the majority of the bandwidth (due to the fixing), and this meant there was a greater difference between the refractive index of the quartz (2.1) and that of the adipose (e.g., 1.5 at 1 THz when fixed compared to 1.6 when it was fresh). From Fresnel theory, this increased difference in refractive indices resulted in a greater reflected amplitude.

As the fixing time increased for the muscle, three main changes were apparent. A small peak started to appear preceeding the trough, and the width and magnitude of the trough decreased. These changes can also be explained by considering the effects of the formalin on the refractive index and absorption coefficient of the muscle. For the muscle, the formalin significantly reduced both the refractive index and the absorption coefficient. Before fixing, the refractive index of

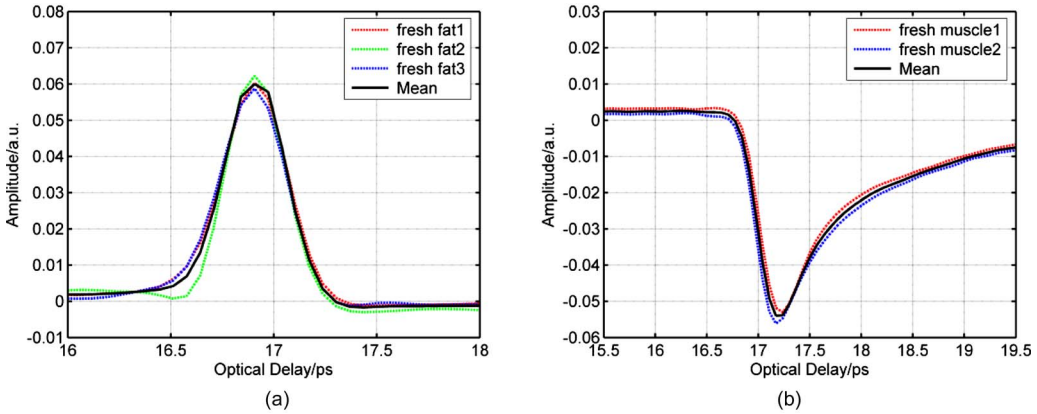


**Fig. 5** The deconvolved waveforms for fresh samples of (a) adipose tissue and (b) skeletal muscle.

the fresh muscle was greater than that of quartz (2.1) over the whole of the frequency range measured. The fixing reduced the refractive index so much that the refractive index became lower than that of quartz at higher frequencies, and this was the cause for the small peak, which appeared and increased as the fixing time was increased. As the the refractive index and absorption coefficient were reduced they became closer to the optical properties of the quartz. This meant that the reflected waveform was not as intense. Additionally, because the absorption coefficient was reduced there was less broadening of the trough (as more of the higher frequency components were preserved), and thus, we observed a narrower reflection. Therefore, the formalin fixing can significantly affect the THz properties of samples such that they are apparent in both the frequency and time domain.

Figures 7(a) and 7(b) present the deconvolved THz waveforms for fresh and fixed tissue, respectively. In both figures, we can see clear differences between the adipose tissue and muscle waveforms; however, the differences are bolder for the fresh sample. When investigating a biological sample, we typically look at an image of the whole sample, and plot particular properties in the image. For instance, we may plot at each pixel the maximum or minimum reflected waveform amplitude, or the refractive index at 1 THz.

Figure 8(b) is the THz image corresponding to the area of interest in the photograph of the fixed tissue in Fig. 8(a). To form the image, the maximum amplitude of the deconvolved waveform is plotted on a false-color scale. The more blue regions have higher maximum waveform amplitude, and the redder regions have lower maximum waveform amplitude. The dark blue areas in the image correspond to where there was no sample on the quartz window—these waveforms have the highest amplitude because the reflected pulses are identical to the reference pulses. We can also see contrast between the adipose tissue and the skeletal muscle: the region of this image corresponding to the adipose tissue is pale blue, but the rest of the image is more yellow/red. This is because the deconvolved waveforms from the adipose tissue have the same phase as the reference waveform, whereas the deconvolved waveforms from the muscle undergo a phase change due to the higher refractive index of the muscle relative to the quartz. Therefore, despite reducing the differences in both the time and frequency domain properties of the adipose and muscle, we were still able to distinguish the adipose tissue from the muscle in Fig. 8(b).

## 4 Conclusion

In summary, we have used THz pulse imaging and reflection spectroscopy to determine the time- and frequency-dependent optical properties of tissue undergoing formalin fixation. The THz properties were affected by the formalin fixing as it (a)

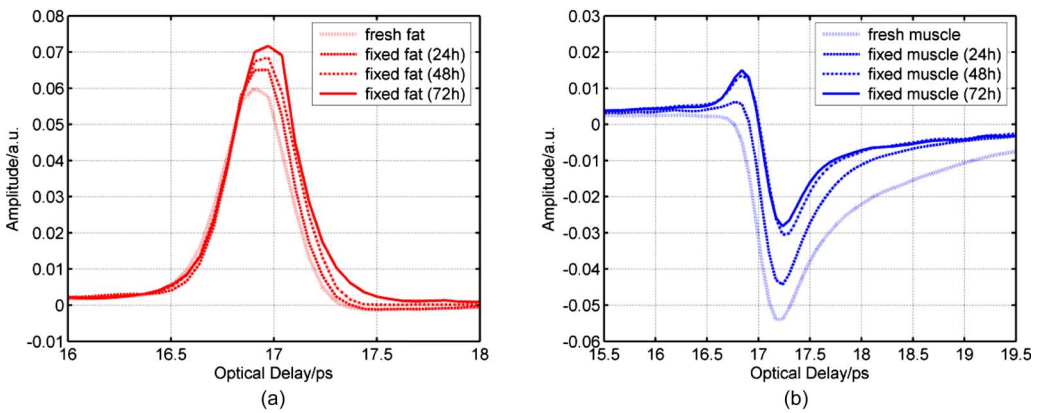


**Fig. 6** The deconvolved mean waveforms for (a) adipose tissue and (b) skeletal muscle as the fixing time progressed.

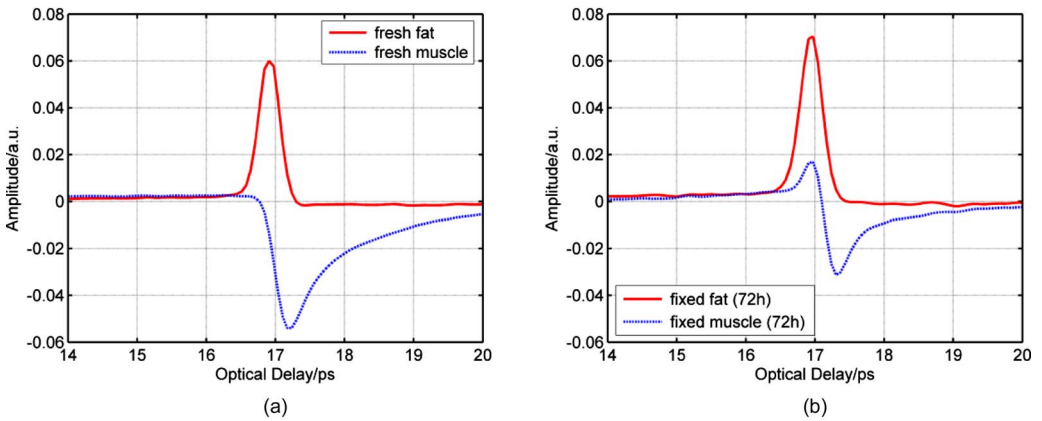


**Fig. 7** The deconvolved waveforms for (a) fresh and (b) fixed white adipose tissue and skeletal muscle.

displaced water molecules and (b) introduced new intermolecular interactions between the sample and the formalin. It is well known that THz radiation is sensitive to hydrogen bonding, and thus, water content changes. Additionally, we infer that the newly introduced intermolecular interactions may also have contributed to the THz response.

In our example study of adipose tissue and muscle, the fixing process reduced the differences between the absorption coefficient and refractive index. However, in this case, there were still significant enough differences between the parameters for the two tissue types to be distinguished. In cases where the differences between tissues are more subtle, this may not be the case, and formalin fixing may prevent THz imaging from being able to distinguish the samples. Therefore, when investigating biomedical applications of TPI, it is very important to understand the composition of biological samples and be aware of how formalin fixing may reduce or enhance THz image contrast.

## *Acknowledgment*

We thank Andreas Thoman of the University of Freiburg, Germany, for assisting with the spectroscopy measurements of formalin. The authors gratefully acknowledge partial financial support for this work from the Research Grants Council of the Hong Kong Government and the Shun Hing Institute of Advanced Engineering, Hong Kong.

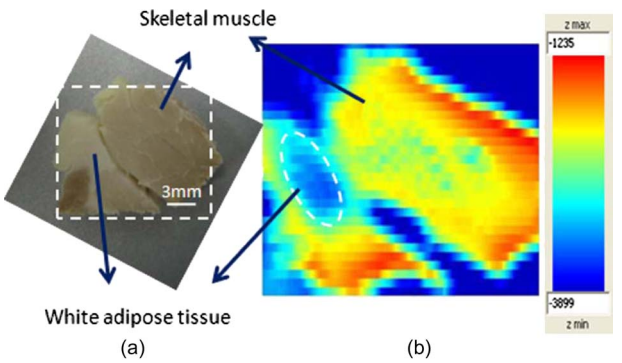


**Fig. 8** (a) Photograph of the fixed tissue. (b) THz image corresponding to the area of interest within the square in (a).

## *References*

1. D. H. Auston, "Picosecond optoelectronic switching and gating in silicon," *Appl. Phys. Lett.* **26**, 101–103 (1975).
2. P. F. Taday, I. V. Bradley, D. D. Arnone, and M. Pepper, "Using terahertz pulse spectroscopy to study the crystalline structure of a drug: A case study of the polymorphs of ranitidine hydrochloride," *J. Pharm. Sci.*, **92**(4), 831–838 (2003).
3. V. P. Wallace, P. F. Taday, A. J. Fitzgerald, R. M. Woodward, J. Cluff, R. J. Pyeand, and D. D. Arnone, "Terahertz pulsed imaging and spectroscopy for biomedical and pharmaceutical applications," *Faraday Discuss.* **126**, 255–263 (2004).
4. E. Pickwell, V. P. Wallace, B. E. Cole, S. Ali, C. Longbottom, R. Lynch, and M. Pepper, "A comparison of terahertz pulsed imaging with transmission microradiography for depth measurement of enamel demineralisation *in vitro*," *Caries Res.*, **41**, 49–55 (2007).
5. R. M. Woodward, V. P. Wallace, R. J. Pye, B. E. Cole, D. D. Arnone, E. H. Linfield, and M. Pepper, "Terahertz pulse imaging of *ex vivo* basal cell carcinoma," *J. Invest. Dermatol.*, **120**, 72–78 (2003).
6. A. J. Fitzgerald, V. P. Wallace, M. Jimenez-Linan, L. Bobrow, R. J. Pye, A. D. Purushotham, and D. D. Arnone, "Terahertz pulsed imaging of human breast tumors," *Radiology*, **239**, 533–540 (2006).
7. Y. C. Shen, T. Lo, P. F. Taday, B. E. Cole, W. R. Tribe, and M. C. Kemp, "Detection and identification of explosives using terahertz pulsed spectroscopic imaging," *Appl. Phys. Lett.* **86**(24), 241116 (2005).
8. M. C. Beard, G. M. Turner, and C. A. Schmuttenmaer, "Terahertz spectroscopy," *J. Phys. Chem. B* **106**, 7146–7159 (2002).
9. R. H. Clothier and N. Bourne, "Effects of THz exposure on human primary keratinocyte differentiation and viability," *J. Biol. Phys.* **29**, 179–185 (2003).
10. J. T. Kindt and C. A. Schmuttenmaer, "Far-Infrared dielectric properties of polar liquids probed by femtosecond terahertz pulse spectroscopy," *J. Phys. Chem.* **100**, 10373–10379 (1996).
11. K. J. Tielrooij, R. L. A. Timmer, H. J. Bakker, and M. Bonn, "Structure dynamics of the proton in liquid water probed with terahertz time-domain spectroscopy," *Phys. Rev. Lett.* **102**, 198303 (2009).
12. W. Withayachumnankul, G. M. Png, X. X. Yin, S. Atakaramians, I. Jones, L. Hungyen, B. Seam Yu Ung, J. Balakrishnan, W. H. Brian Ng, B. Ferguson, S. P. Mickan, B. M. Fischer, and D. Abbott, "T-Ray sensing and imaging," in *Proc. IEEE* Vol. **95**, pp. 1528–1558 (2007).
13. C. J. Strachan, P. F. Taday, D. A. Newnham, K. C. Gordon, J. A. Zeitler, M. Pepper, and T. Rades, "Using terahertz pulsed spectroscopy to quantify pharmaceutical polymorphism and crystallinity," *J. Pharm. Sci.*, **94**, 837–846 (2005).
14. D. M. Mittleman, M. C. Nuss, and V. L. Colvin, "Terahertz spectroscopy of water in inverse micelles," *Chem. Phys. Lett.*, **275**, 332–338 (1997).
15. M. Walther, B. M. Fischer, M. Schall, H. Helm, and P. U. Jepsen, "Far-infrared vibrational spectra of all-trans 9-cis and 13-cis retinal measured by THz time-domain spectroscopy," *Chem. Phys. Lett.*, **332**, 389–395 (2000).
16. B. M. Fischer, M. Hoffmann, H. Helm, R. Wilk, F. Rutz, T. Kleine-Ostmann, M. Koch, and P. U. Jepsen, "Terahertz time-domain spec-

troscopy and imaging of artificial RNA," *Opt. Express* **13**, 5205–5215 (2005).
17. B. M. Fischer, H. Helm, and P. U. Jepsen, "Chemical recognition with broadband THz spectroscopy," in *Proc. IEEE* Vol. **95**, pp. S246–S253 (2007).
18. R. M. Woodward, V. P. Wallace, D. D. Arnone, E. H. Linfield, and M. Pepper, "Terahertz pulsed imaging of skin cancer in the time and frequency domain," *J. Biol. Phys.* **29**, 257–261 (2003).
19. E. Pickwell, V. P. Wallace, A. J. Fitzgerald, B. E. Cole, R. J. Pye, T. Ha, and M. Pepper, "Simulating the response of terahertz radiation to human skin using *ex vivo* spectroscopy measurements," *J. Biomed. Opt.* **10**, 064021 (2005).
20. V. P. Wallace, A. J. Fitzgerald, E. Pickwell, R. J. Pye, P. F. Taday, N. Flanagan, and T. Ha, "Terahertz pulsed spectroscopy of human basal cell carcinoma," *Appl. Spectrosc.* **60**, 1127–1133 (2006).
21. S. Y. Huang, Y. X. J. Wang, D. K. W. Yeung, A. T. Ahuja, Y. T. Zhang, and E. Pickwell-MacPherson, "Tissue characterisation using terahertz pulsed imaging in reflection geometry," *Phys. Med. Biol.* **54**, 149–160 (2009).
22. R. C. Grafstrom, A. Fornace, Jr., and C. C. Harris, "Repair of DNA damage caused by formaldehyde in human cells," *Cancer Res.* **44**, 4323–4327 (1984).
23. P. Knobloch, K. Schmalstieg, M. Koch, E. Rehberg, F. Vauti, and K. Donhuijsend, "THz imaging of histo-pathological samples," *Proc. SPIE* **4434**, 239–245 (2001).
24. E. Pickwell, "Biological applications of terahertz pulsed imaging and spectroscopy," Ph.D. Thesis, Cambridge Univ. (2005).
25. E. Pickwell, B. E. Cole, A. J. Fitzgerald, M. Pepper, and V. P. Wallace, "*In vivo* study of human skin using pulsed terahertz radiation," *Phys. Med. Biol.* **49**, 1595–1607 (2004).
26. S. Y. Huang, E. Pickwell-Macpherson, and Y. T. Zhang, "A new data processing scheme to reduce variations in terahertz pulsed imaging," in *Proc. of Int. Workshop on Wearable and Implantable Body Sensor Networks (BSN 2008), with 5th Int. Summer School and Symp. on Medical Devices and Biosensors*, Hong Kong, pp. 236–239, IEEE, Piscataway, NJ (2008).
27. D. M. Mittleman, *Sensing with Terahertz Radiation*, Springer, Berlin (2003).
28. B. E. Cole, R. Woodward, D. Crawley, V. P. Wallace, D. D. Arnone, and M. Pepper, "Terahertz imaging and spectroscopy of human skin, *in vivo*," *Proc. SPIE* **4276**, 1–10 (2001).
29. M. H. Hofker and J. V. Deursen, *Methods in Molecular Biology*, Humana Press, NJ (2002).
30. L. C. Junqueira, *Basic Histology: Text & Atlas*, McGraw-Hill, New York (2005).
31. D. W. Cromey, *Formaldehyde fixatives*, Southwest Environmental Health Sciences Center, Univ. of Arizona (2004).
32. L. Johannes and V. H. Robert, *Applied Statistics for Engineers and Physical Scientists*, Prentice Hall, Englewood Cliffs, NJ (2009).
33. M. R. Stringer, D. N. Lund, A. P. Foulds, A. Uddin, E. Berry, R. E. Miles1, and A. G. Davies, "The analysis of human cortical bone by terahertz time-domain spectroscopy," *Phys. Med. Biol.* **50**, 3211–3219 (2005).
34. C. L. Nie, W. Zhang, D. Zhang, and R. Q. He, "Changes in conformation of human neuronal tau during denaturation in formaldehyde solution," *Protein Peptide Lett.* **12**, 75–78 (2005).
35. J. F. Walker, *Formaldehyde*, Reinhold, New York (1964).
36. C. H. Fox, F. B. Johnson, J. Whiting, and P. P. Roller, "Formaldehyde fixation," *J. Histochem. Cytochem.* **33**, 845–853 (1985).
37. A. Younge, C. F. Van Niekerk, and S. Mogotlane, *Juta's Manual of Nursing*, Juta & Co., Cape Town, South Africa (2003).